FACTORS LIMITING THE OPERATION OF STRUCTURES UNDER HIGH GRADIENT*

S. O. SCHRIBER, AT-DO, MS H811
LOS ALAMOS NATIONAL LABORATORY, LOS ALAMOS, NM 87545

Summary

Factors limiting the operation of rf structures under high-gradient conditions are described. Included are recent rf measurements at laboratories in Europe, Asia, and North America and how these measurements relate to earlier data as exemplified by the use of the Kilpatrick criterion (Kp). Operation limitations will cover mechanical, geometry, thermal, and surface constraints and the associated impact on structure design, fabrication, and material selection. Generally, structures operating continuous wave (100% duty factor) appear to be limited to peak surface fields at about twice the Kilpatrick limit, whereas pulsed structures operating with pulse lengths less than a millisecond can attain peak surface fields five times the Kilpatrick limit.

Introduction

Interest in operating accelerating structures with high rf fields has been driven by a number of reasons, including those listed below:

- Shorter and smaller accelerators
- Restrictions on available space
- Improved performance, in particular for injectors
- Economics, particularly when beam powers exceed structure powers
- Beam-handling improvements
- Efficient systems in terms of temporal, operation, and response characteristics

If 500 MeV/m accelerating gradients were possible, a 50-GeV accelerator could be built in 100 m compared to 5000 m required for typical 10 MeV/m currently available—a considerable savings but at the expense of rf power and cooling.

An understanding of the mechanisms and related factors for rf field breakdown in rf structures could lead to improved operation, the use of preferred materials, the selection of operating environments, and the ability to operate economically (and safely) close to a well-selected choice of system limitations. A detailed investigation of breakdown phenomena could lead to a sufficient understanding of the surface physics, chemistry, and metallurgy to make significant advances in the state of our technology. For these reasons, it is important that a multidisciplinary approach be taken in the research and development activities. The overlap in technology exchange between superconducting and room-temperature structure studies is just as important for both study areas as it is for studies of dc and rf breakdown.

For many years the Kilpatrick limit[1] has been used to express limitations in operating rf surfaces at very high rf fields. Kilpatrick analyzed data available in the mid-fifties and determined a limit at which there was a high probability of field breakdown or arcing between surfaces. Operation below this level would generally be trouble free. Since then vacuum systems have improved and higher rf surface fields have been achieved—factors of 5 or better have been observed. A significant improvement was the introduction of oil-free vacuum pumps, which eliminated the need for diffusion pumps and the associated oil contamination of vacuum surfaces. Accelerator designers and operators talk of a structure performing at "X" times the Kp as a mechanism for comparing data between different accelerator groups and for different frequency regimes. The following formula is a simplified reordering for the case where the gap effect is negligible:

$$f(\mathrm{MHz}) = 1.643\,E^2(\mathrm{MV/m})\exp(-8.5/E) \quad .$$

Above a surface field E, the probability of breakdown is high for an rf structure operating at frequency f. Typical values are 11.5 MV/m at 108 MHz, 15.1 MV/m at 216 MHz, 20 MV/m at 432 MHz, and 50 MV/m at 3000 MHz. If high fields are required, as high a frequency as possible should be chosen, subject to the constraints of fabrication (physical limitations), available rf power sources, and required beam dimensions for propagation and containment of charged particle beams.

The rf fields available for accelerating charged particle beams are related to the rf surface fields by geometric factors. Proper design of the cavity geometry is important for attaining high fields, as is the frequency choice. Attention should be paid to cooling the rf surfaces if degradation of performance is to be avoided—degradation from increases in surface temperature such as a loss of rf efficiency or a change in physical dimensions.

Figure 1[2] shows the regimes available for operating an rf structure safely. Operation would be difficult above the lines drawn for three different effects. The breakdown limit will be the subject of the rest of this paper. This limit is the predominant effect up to about 50 GHz—below which is the usual operating regime for accelerators. Above this frequency two other effects become dominant: a surface phenomenon related to melting the rf surface from the high rf currents induced in several skin depths of the cavity walls, and the formation of plasma close to the surface.

This paper describes results obtained with room-temperature systems since the 1984 Linac Conference. Other papers at this conference describe the status of superconducting technology. Also described is the outcome of discussions at a mini-workshop, organized by the author, on limitations to high surface fields (SLAC, September 1985). Headings used below refer to the institution at which most of the work took place. Because of space limitations, work at some institutions will be mentioned briefly, other work not at all. To provide an overview of effects and technology status, specific topics have been highlighted.

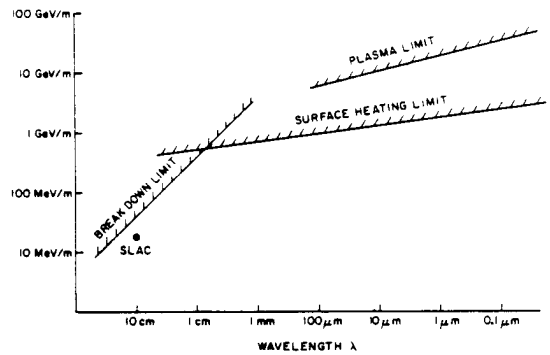

Fig. 1. Operating limitations versus wavelength.

Chalk River Nuclear Laboratory

Hutcheon et al.[3] performed a number of experiments with a 270-MHz RFQ "Sparker" cavity that was designed to determine cw limitations. The four-vane geometry shown in Fig. 2 was instrumented for visual, thermal, rf, and radiation measurements. High-power rf was delivered to the structure with an rf loop that was locally compensated by adding material around the periphery of the coupling hole. Field uniformity from quadrant to quadrant was within ±3% as measured by standard bead-pull techniques. The vanes and the outer walls were fabricated from solid OFHC copper, with internal channels for flood cooling. The all-brazed (hydrogen furnace) structure attained 90% of the theoretical Q value. The TE_{211} quadrupole mode frequency was 266.7 MHz at 22°C with no cooling water flow (TE_{111} dipole modes at 270.5 and 264.8 MHz). Note that the end walls in Fig. 2 were far removed from the vanes to eliminate end-wall effects. A bakeout at 90°C, limited by some of the attached components, resulted in a background pressure of 10^{-5} Pa.

Initial operation resulted in vacuum excursions to 10^{-3} Pa with tiny "glow points" visible on the vanes, not all at the highest field locations—some of them in fact at relatively low field spots. Glow points became visible at the 1- to 2-kW drive level, corresponding to about 1/3 to 1/2 * Kp. As rf drive levels increased, so did the number and light intensity from each glow point. Some disappeared, some disappeared and reappeared, while others remained at what seemed to be the same location. Care had been taken to ensure no contamination of the RFQ components by employing suitable clean techniques during assembly and initial vacuum pump down. Perhaps some of the glow points were associated with impurities, dielectric inclusions, or other surface imperfections. The situation lacked some of the high-quality clean-room techniques used for assembling superconducting structures. Impurities

*Work supported by U.S. Department of Energy.

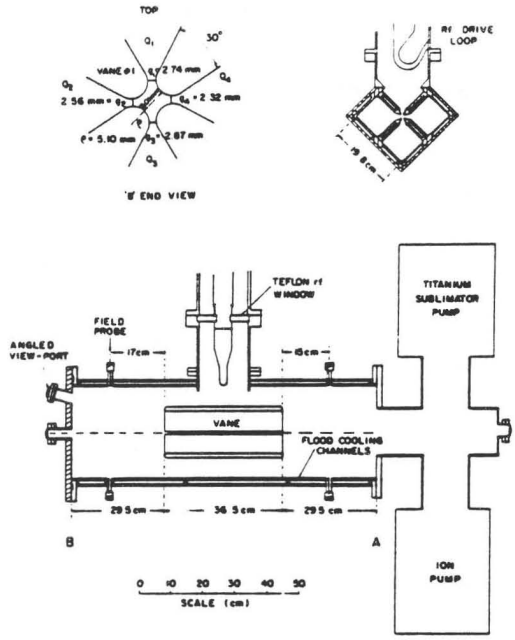

Fig. 2. Schematic of RFQ sparker.

on surfaces of either superconducting or room-temperature devices can lead to high field limitations—the consequences for superconducting structures being much more severe.

Because of the care taken during assembly and the procedures used during rf field conditioning, the RFQ cavity reached high field operation relatively quickly. The criteria employed were the usual ones adopted by most accelerator institutions: (1) vacuum excursions from surface breakdown were held to acceptable levels and (2) energy deposited on the surfaces from a major breakdown arc was minimized by a quick shutdown of the high-power rf system. The sequence followed for first high-power operation was a combination of pulsed (10 pps at 0.15-ms pulse length) and cw operation. The initial 15 hours required to attain acceptable high field operation consisted of 2 hours pulsed to 1.6 * Kp, 2-1/2 hours cw to 1.3 * Kp, 1-1/2 hours cw to 1.5 * Kp, 4 hours pulsed to 2 * Kp, and 5 hours cw to 2.2 * Kp. During the following months, operation at 3 * Kp pulsed (0.25-ms pulse length) and 2.3 * Kp cw (about 50 kW) was routinely achieved. The shorter the pulse length, the higher the field that could be sustained without significant breakdown. Some general characteristics follow: 1-MHz frequency shift from no rf input to cw operation at 2 * Kp, 10^{-4} Pa vacuum with rf fields, VSWR 1.17 overcoupled, and 9700 unloaded quality factor.

Vanes were inspected and cleaned with acetone, trichloroethane, and ethanol after several months of operation. Visual inspection showed no signs of erosion, a significant change from what has been common with most copper-plated surfaces. A critical inspection of the surface by surface chemistry techniques showed no significant change. Reconditioning to high fields went much faster and it was observed that the number of glow points decreased by about an order of magnitude. Some of the glow points appeared to be at the same location as before—to within the accuracy of the visual information stored on video tapes from the TV camera system.

Temporal characteristics of the light emitted during pulsed operation were measured with a low-gain photomultiplier tube that was calibrated off-line to have an 0.3-ms rise-time. At various rf power levels, the light rise time (10 to 90% level) was 1.3 ms, independent of duty factor or pulse length. The intensity remained constant to the end of the rf pulse, at which time the light decay time (90 to 10% level) was 0.8 ms. These times are much longer than the 8-μs rise time (10 to 90% level) for the rf fields and are probably associated with thermal effects. Figure 3 shows modulation of the light output from a large frequency modulation excursion used for this measurement only, by the automatic frequency control circuit (100-Hz modulation about the resonant frequency). Emitted light is a sensitive measure of cavity conditions—compare the light to the cavity quadrant probe of Fig. 3. Figure 4 shows the relative light intensity measured as a function of the rf fields in the cavity. Note the steep functional dependence and the onset at about 1 * Kp.

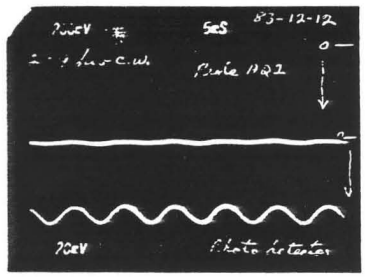

Fig. 3. Modulation of light intensity (lower trace) and rf field in RFQ (upper trace) at 29.9-kW cw operation.

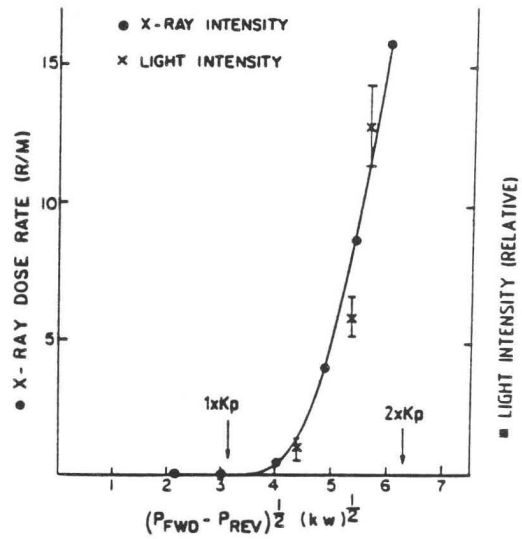

Fig. 4. X-ray and light intensity (measured outside of quartz window) versus square root of input power.

Light output can be used to determine a threshold for cavity breakdown. For any particular operation, a specific light intensity could be determined that, if exceeded, would result in cavity arcing, independent of pulse length. For pulse lengths greater than the 1.3-ms light rise time, no rf pulse-length effects were observed—operation was essentially limited to that for cw operation. For pulse lengths shorter than 1.3 ms, the peak rf field attained was related to the light threshold. Because of a fixed light rise time, shorter rf pulses would require higher peak rf fields to reach the light threshold level. This effect agrees with measurements showing that higher peak surface fields can be sustained with shorter rf pulse lengths.

Spectrometric measurements showed the emitted light had a continuous blackbody radiation pattern (T ~ 1200 K). Measurements of absolute light intensity and an estimate of the number of glow points indicated that the points were about 1 to 10 microns in diameter, supporting the thesis that the points could be surface impurities, whiskers, discontinuities, or small imperfections. Heating could be from rf displacement or electron emission currents.

Figure 4 shows x-ray dose rate (measured by a Baldwin-Farmer probe) versus rf field level. A striking similarity to that of the light emission was observed, indicating that both emissions must be related to the same surface effects. X rays were generated by electrons accelerated from vane to vane during the rf cycle. Electron transit time is short, leading to a determination of the intervane voltage by measuring the end point of the x-ray spectrum. Rise and fall times of the x rays were measured to be 1.2 and 0.2 ms, respectively. Similar to light emission, x-ray intensity was independent of duty factor and pulse length when the pulse length exceeded 1.2 ms.

The end point of the x-ray spectrum was measured by a germanium x-ray spectrometer, an accurate method for determining vane-to-vane voltages. Because of the intense radiation field generated, care had to be taken to ensure that the detector and its electronics were not being overloaded and that scattered radiation was minimized at the detector.

This method of measuring vane voltages has been adopted by most institutions operating RFQ accelerators. An average 20-mA electron current between vanes was estimated for operation at 1-3/4 * Kp by calibrating the germanium detector system off-line with a similar geometry and a 70-keV dc electron beam of known beam characteristics.

A microdischarge (small flash of light between adjacent vanes) resulted in a 2-μs collapse (90 to 10%) of the rf fields, followed immediately by the usual 8-μs field rise time. Each microdischarge had an approximate 10-μs loss of field (about 2500 rf cycles), which may be of significance to some accelerator scenarios.

Microdischarges occurred randomly in time and randomly over the length of the vane. Over long (5- to 6-h) cw runs, the following microdischarge rates were observed for the fully conditioned cavity—600/h at 2.3 * Kp, 25/h at 2 * Kp and, 4/h at 1-3/4 * Kp. Detailed examination of the video tapes indicated that many of the microdischarges occurred in the region of the peak rf fields and were either at or in the vicinity of the glow points. Breakdown, sparking or arcing, was associated with a large number of the microdischarges moving about the vane tips in a sustained manner.

Other observations and measurements included

- No noticeable change in high-power operation, as determined by diagnostic devices, when 0.3 mA of 750-keV cw proton beam was transmitted directly through the bore of the device or was directly steered onto the vanes (effective beam impingement or beam loss greater than 3 mA/m).
- Increases in background pressure to 10^{-2} Pa produced no noticeable change in operation for background gases of N_2, Ar, H_2, or air. At pressures above 10^{-2} Pa, microdischarges and breakdown rates increased dramatically. As the pressure increased from 10^{-4} Pa to 10^{-2} Pa, x-ray field levels increased by about 20% except for the case of nitrogen gas, for which a 25% decrease was observed.

University of Frankfurt

Most of the work[4-6] at the University of Frankfurt has been done at 108 MHz using a coaxial λ/4 resonator, shown in Fig. 5, that employed two frequency tuners and two coaxial electrodes, one fixed and one adjustable under vacuum. Electrodes were mechanically polished and ultrasonically cleaned in methanol. The rf field coupling loops were calibrated by x-ray end-point energy from a germanium x-ray spectrometer. Visual observation was by means of a TV camera. A quadrupole mass spectrometer was attached to the vacuum system to measure background gas concentrations during high-power operation.

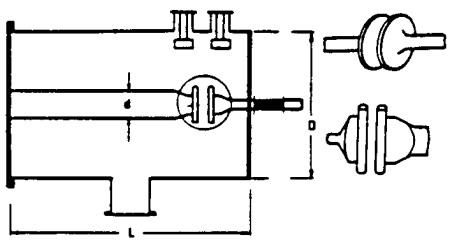

Fig. 5. Schematic of coaxial λ/4 resonator, d = 10 cm, D = 35 cm, and L = 70 cm.

Under pulsed operation, field levels to 4 * Kp were achieved without sparking for pulse lengths up to 1 ms (duty factor to 5%). Under cw conditions, field levels were limited to 2.4 * Kp. Breakdown voltage was dependent on gap width when the gap was small enough to consider gap effects.[1]

Figure 6 shows the 7-cm-diam plane electrode measurements. As pulse length decreased, higher breakdown voltages (U in kV based on a rate of an arc/m) could be sustained. Operation at pulse lengths longer than several ms had an equilibrium level similar to that of cw operation. Smaller gaps supported lower fields. The larger the gap, the closer the operation to Kp. Background vacuum pressure had little effect to 6×10^{-3} Pa.

A comparision of electrode operation demonstrated that a 20-mm-diam cylindrical electrode sustained a voltage (0.5 cm gap) twice that of the plane electrode. A smaller 10-mm-diam electrode displayed a further 10% improvement. Up to 6 * Kp (105 kV versus 17 kV) breakdown voltage was measured with the 20-mm-diam electrode for a 0.1-cm gap. This performance reduced to about 3 * Kp (440 kV versus

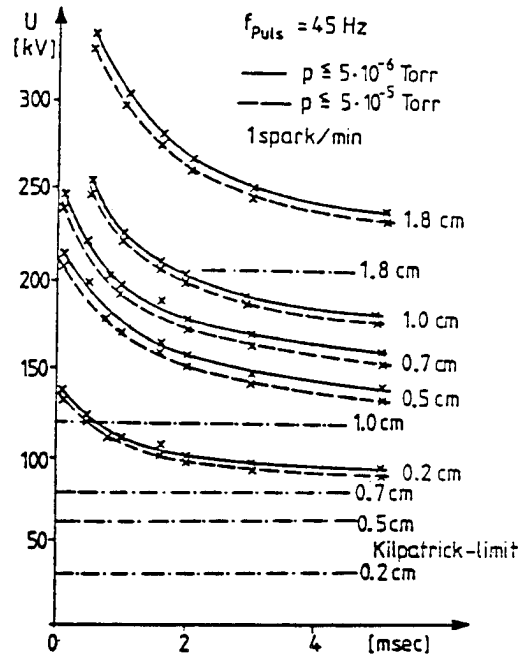

Fig. 6. Breakdown voltage versus pulse length for plane electrodes (7-cm-diam disk) with Kilpatrick limit shown for each gap distance.

147 kV) for a 1.25-cm gap. Geometry plays an important part in voltages sustained in an accelerator. Cavity geometry must be carefully selected to design a system that will support high rf fields. A compromise between rf efficiency, beam loading effects, and rf voltage stand-off must be made.

Some accelerator applications have considered the use of Cs ions (heavy ion fusion) or the use of negative ions, the latter resulting in a small background Cs gas from the ion source for certain source types. Figure 7 displays sparking rate as a function of voltage for operation with and without Cs background gas. A factor of 2 reduction in voltage stand-off capability was noted for pulse lengths from 0.1 to 0.8 ms. This reduction was presumably from the absorption of low work function Cs vapor on the metal surfaces. Sensitivity of this effect to different partial pressures of Cs vapor is still to be investigated. Surfaces returned to their original operating characteristics without Cs after several hours of vacuum pumping.

Electrodes for measurements listed above were made of solid OFHC copper. Machining would be easier if an alloy such as Cr Cu (99.7% Cu, 0.75% Cr, 0.08% Zr) were selected. Material hardness following temperature cycling (associated with fabrication) would also be better than OFHC copper. Unfortunately, breakdown measurements showed that Cr Cu alloy had a 10% lower voltage stand-off capability over a wide range of duty factors and pulse lengths. If a particular application can tolerate a 10% loss in attainable field level, this alloy might be a reasonable choice.

Mass spectrometric measurements showed the typical water components (H and OH), hydrocarbon lines, nitrogen, and carbon dioxide. Hydrogen was the only spectral component that changed noticeably as a

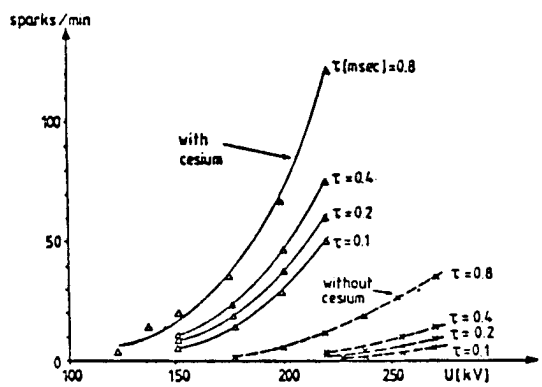

Fig. 7. Sparking rate versus electrode voltage, 0.5% duty cycle, 6 to 45 pps, 0.7 cm gap, 10^{-3} Pa pressure, 83 kV Kilpatrick limit.

function of field. Following cavity conditioning (0.5-cm gap with Kp of 60 kV), the hydrogen partial pressure increases (factors of 5), seen from the 1/3 to 1 * Kp levels, essentially disappeared. A fully conditioned cavity displayed an increase of the hydrogen partial pressure by up to a factor of 5 between the 1 and 1.5 * Kp levels and a significant increase again above 4 * Kp—a lot of the latter associated with arcs.

Preliminary surface examinations following breakdown tests showed that arcing between surfaces resulted in an erosion of the surface with the production of about 0.1-mm-diam craters.

University of Mainz

Staff at the University of Mainz have been working on a three-stage microtron to obtain 840-MeV cw electron beams for research purposes. The accelerating structures in each of the microtons (14- and 180-MeV intermediate stages) and the injector are based on a 2450-MHz on-axis coupled linac developed[7] at the University of Mainz on the basis of work[8] at CRNL. The cw linac had to be designed carefully with considerations of rf efficiency, geometry, higher order mode excitation, cooling, inter-cavity coupling and fabrication methods. An associated experiment in collaboration with CRNL was undertaken to determine the limits to operating the linac under high-power rf conditions.

Although the linac (three accelerating cells, two coupling cells) was operated at maximum surface fields less the 1/3 * Kp, glow points were visible on the noses of the shaped accelerating cells as viewed along the structure axis. A 1/3 * Kp limit was determined,[9] based on thermal effects described below. This operating level corresponded to 3.5 MeV/m average accelerating gradient with a related power level of 210 kW/m—heat that had to be removed from the structure (see Fig. 8). Best operation of such a biperiodic structure will occur if the stop-band gap between the two bands of the frequency dispersion spectra remains relatively small (< 0.02% of operating frequency) over all operating conditions.

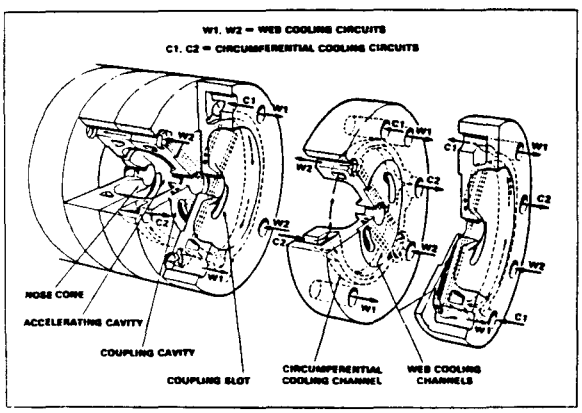

Fig. 8. Schematic of on-axis coupled cavity showing cooling circuits.

Because of unequal heating of the webs (heat from accelerating cell side, very little from coupling cell side), web movement can lead to a significant stop-band gap. This frequency shift is related to the high relative sensitivity of the coupling cell to on-axis gap changes. Figure 9 shows the stop-band gap as a function of input power for circumferential cooling only (maximum web stress) and for web plus circumferential cooling. For the latter case, operation to 210 kW/m was acceptable.

Measurements of the stop-band gap (by measuring all passband modes) as a function of power for circumferential cooling only showed that for powers less than 70 kW/m the stop-band gap returned to its zero power value after each cycle. At higher power levels, a permanent distortion was introduced. For example, a measured, permanent, 0.5-MHz stop-band gap was introduced after operation to 100 kW/m (corresponding 2.5-MHz stop-band gap). This distortion (thermal limit) was caused by taking some of the web past the copper yield stress and introducing a permanent deformation. Web cooling allowed one to reach 210 kW/m before these effects became important.

KEK, Japan High Energy Physics Laboratory

In studies[10] of a 201-MHz RFQ for accelerating H^- from 50 keV to 750 keV, electropolishing of solid copper resulted in good rf conductivity

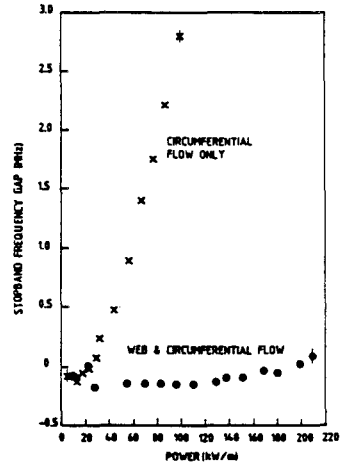

Fig. 9. Stop-band frequency gap versus input power for two cooling situations.

and relatively high breakdown levels. Cross-sectional views of surfaces before and after polishing showed significant surface-roughness reductions. Polishing to depths of 25 to 50 μm seemed to be optimum. DC tests of OFHC copper RFQ vane simulation pieces showed that about 2.4 * Kp was attainable for no electropolishing, a 25-μm polish, a 50-μm polish, and a 100-μm polish.

Different materials (metals and dielectrics) are being investigated[11] for performance, with attention to dissolved gases, surface structure, local heating, multipactoring, grain sizes, voids, and polishing techniques.

Lawrence Berkeley Laboratory

The Bevatron 200-MHz Alvarez linac injector has been operating (1 ms, about 2 pps) at about 1 * Kp for more than 10 years. Recently[12] it was opened for a rebuild. A noticeable amount of copper was lying at the bottom of the tank in the location of the first 10 drift tubes. These drift tube surfaces showed a significant amount of pitting or erosion. In addition, multipactor patterns were seen on the outer wall. The solid-copper drift tubes were soft soldered and Ag plated. The Ag plate peeled off within 2 weeks of initial operation, and the soft solder was eroded out of the joints, especially from the first few drift tubes.

Kennedy[13] has investigated RFQ electrode surfaces by placing cylindrical samples 0.25 mm from an electropolished stainless steel electrode with a 1.3-cm radius of curvature, the system energized in vacuum by a 60-Hz power source. Electroless Ni surfaces held off voltage about 30% better than bare steel, which itself was about 20% better than a 0.005-mm Cu-plated (cyanide copper electroplate) surface. After about 180 sparks, the 0.005-mm Cu plate eroded so severely that bare steel was exposed—determined by a scanning electron microscope examination. A thicker, 0.05-mm Cu-plated surface showed the same general traits, with more sparks required to reach the bare-steel backing.

The better performance of the electroless Ni surface has been attributed to a small amount of contained P that increased the material mechanical strength. The increase in strength may prevent tearing out of whiskers and subsequent sparking.

A joint LBL/LLNL two-beam accelerator program[14] involving a seven-cell 35-GHz structure (see Fig. 10, based on the SLAC $2\pi/3$ mode

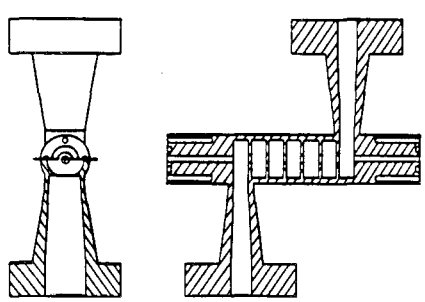

Fig. 10. Schematic of two-beam high-gradient test structure.

design) has attained 1400-MV/m surface fields (about 8 * Kp) for 80 MW of pulsed input power (10 ns, 1 pps). Surface finish of the 6.7-mm-diam structure formed from Cu electroforming and etch removal of Al rings is excellent at several microinches.

Stanford Linac Accelerator Centre

RF breakdown studies have been performed on a seven-cell 2856-MHz structure similar to that of Fig. 10, except that the cavity has an 8.2-cm diam and operates in a π standing wave mode. Surface fields of 300 MV/m (6 * Kp) were reached[15] for operation at 37-MW peak (2.5-ms pulse, 120 pps). Associated with this operation were high radiation fields on-axis from about 25-mA peak, 10-MeV electrons. Because of the intense and energetic electrons, structure end plates or windows must be designed carefully. Fowler-Nordheim plots[16] were used to display rf processing. Surface electron emission under the influence of strong electric fields can be plotted, I (electron emission current)/E^2 (Electric field across surfaces), as a function of 1/E to determine a surface enhancement factor β that should improve with conditioning.

$$\ln(I/E^2) = -\frac{A}{\beta E} + \ln(B\beta^2\varnothing_s)$$

where A and B are constants and $\varnothing_s$ is the surface area. The factor β can be determined from the slope or intercept of this straight line. Figure 11 shows typical Faraday cup results for the 2856-MHz cavity. Lines 1 to 4 showing β improvements from 140 to 102 were based on (1) initial conditions after a 250°C bakeout, (2) several weeks of rf conditioning, (3) argon processing at 10^{-3} Pa, and (4) conditioning after argon processing.

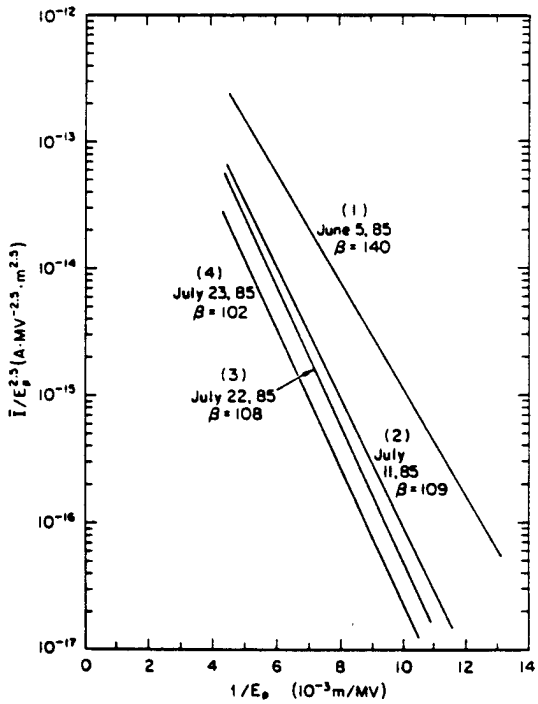

Fig. 11. Modified Fowler-Nordheim plots for the SLAC disk-loaded structure.

Varian

Figure 12 shows Tanabe's[17] setup for testing different materials under controlled conditions with a half-cell coupled-cavity. One of the 3-GHz cavity results (4.4-μs pulse at 200 pps) showed attainment of 250-MV/m (5 * Kp) surface fields for three cavity nose lengths. Peak surface field was the same for the three geometries but the beam accelerating field changed by more than a factor of 2—demonstrating the importance of a design optimization that trades rf efficiency for available accelerating field.

Recent measurements in conjunction with SLAC for a 5-GHz cavity showed 450 MV/m surface fields (7 * Kp). Anomalous effects were observed [18] for high-power operation of 3-GHz structures at −197°C. The

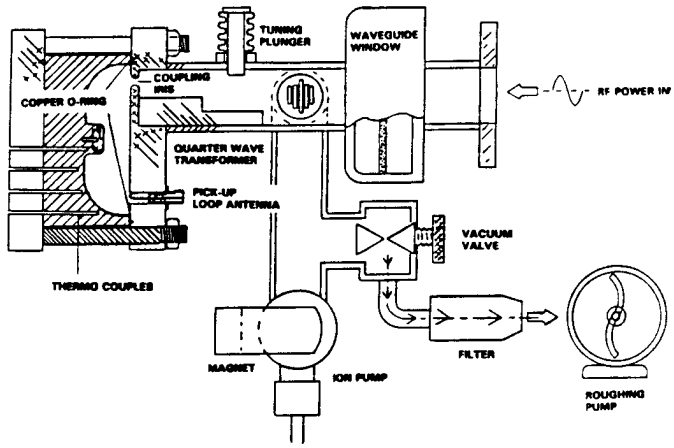

Fig. 12. Cross-sectional view of test cavity system.

Q enhancement by a factor of 2.7 from room temperature to −197°C observed for low power operation was lost for high power operation. Further studies on this effect are planned.

Breakdown level was not enhanced from diamond polishing nor from electropolishing of surfaces, was independent of pulse repetition rate (70 to 300 pps) and cooling temperature (−180° to 40°C), was the same for surfaces of stainless steel, aluminum, titanium, solid OFHC copper and Cu-plated steel, was not enhanced by Ti coatings, and actually decreased with Ni plating.

Summary and Conclusions

Significant amounts of information are available on the limitations to operating rf systems at high fields. A better understanding of what is happening on the surface, in detail, and what improvements are possible is the impetus for future activities. The observables, such as x-ray and light emission, have proved to be important diagnostic tools.

A number of ideas explain surface phenomena that limit high field operation. These include surface heating from ion bombardment, electron emission from surface imperfections and vaporization effects, and the clump hypothesis leading to transfer of significant amounts of material. Clean surfaces, free of impurities and defects, are preferred. Limitations seem to be related to adsorbates, oxides, dust, inclusions, surface defects, dielectric clumps, and eroded trouble spots. Material choice, and subsequent cleaning techniques during processing and fabrication are important considerations.

To reduce the problems from eroded locations, one should employ conditioning procedures that minimize the production of eroded spots and subsequent enlargement or degrading of the eroded areas. A procedure that surveys gas evolution and field emission during operation should be adopted. Attention should be paid to details of the vacuum system, possible baking, and cleaning with an inert background gas such as argon. It is an absolute necessity to minimize arcing or sparking on the surfaces. A conditioning technique using both pulsed and cw operation is especially effective, as long as the microdischarge rate is kept reasonable.

Thermal characteristics and limitations caused by taking material beyond yield stresses should be considered in the design of rf systems. An important aspect is the selection of the cavity geometry and the means of cooling the rf surfaces.

Design of rf sytems should minimize the production of x rays and ultraviolet radiation—if not totally possible, then minimize the impingement of these radiations on surfaces experiencing high stresses and surfaces prone to damage from these radiations.

Future activities will include studies of surface coatings such as thin dielectrics or composites, shorter pulses to attain higher surface fields, imbedded impurities to study local surface effects, microscopic surface investigations under high power rf operation and a detailed study of the anamalous cryogenic (liquid nitrogen) effect at 3000 MHz.

Acknowledgments

The author would like to thank R. M. Hutcheon, G. E. McMichael, J. M. Potter, H. Klein, A. Schempp, P. Junior, H. Euteneur, H. Herminghouse, J. P. Labrie, G. O. Bolme, E. Tanabe, K. Kennedy, J. Staples, J. W. Wang, G. A. Loew, D. Hopkins, and R. W. Hamm for participating in

discussions on this topic and for information supplied that has been used in this paper. The results and data presented are based on the author's interpretation of these discussions and information. A final thanks to Betty Jane Ferandin for her patience and perseverance.

References

1. W. D. Kilpatrick, "Criterion for Vacuum Sparking Designed to Include Both RF and DC," Rev. Sci. Instr., 28, No. 10, 824 (1957).
2. R. B. Palmer, "Near Field Accelerators," Proc. of 1982 Laser Accel. of Part. Conf., AIP Conf. Proc. No. 91, 179 (1982).
3. R. M. Hutcheon et al., "Operation of a cw High Power RFQ Test Cavity: The CRNL Sparker," Gesellschaft fr Schwerionen-forschung report No. GSI-84-11, 74 (1984).
4. A. Gerhard et al., "RF Sparking Experiments," IEEE Trans. on Elect. Insulation, EI-20, No. 4, 709 (1985).
5. A. Gerhard et al., "RF Sparking Experiments," Proc. of XIth Int. Symp. on Discharges and Elect. Insulation in Vacuum, Berlin, Germany, 37 (1984).
6. A. Schempp et al., "RFQ Development and Sparking Experiments in Frankfurt," Proc. of Int. Symp. on Heavy Ion Fusion, Washington, DC, May 1986—to be published.
7. H. Euteneuer, H. Schler, "Experiences in Fabricating and Testing the RF-Sections of the Mainz Microtron," these proceedings.
8. S. O. Schriber, E. A. Heighway, and L. W. Funk, "Beam Tests with S-Band Standing Wave Accelerators Using On-Axis Couplers," Proc. of 1972 Linac, Conf., Los Alamos Scientific Laboratory report no. LA-5115, 140 (1972).
9. J. P. Labrie, H. Euteneur, "Power Handling Capability of Water Cooled CW Linac Structures," to be published in NIM.
10. T. Kato et al., "RFQ Development at KEK," Gesellschaft fr Schwerionenforschung report No. GSI-84-11, 321 (1984).
11. J. Tanaka, "Advanced Technology Recently Developed at KEK for Future Linear Colliders," these proceedings.
12. J. Staples, private communication, 1985.
13. K. Kennedy, private communication, 1985.
14. A. M. Sessler, "The Two Beam Accelerator," these proceedings.
15. J. W. Wang and G. A. Loew, "Measurements of Ultimate Accelerating Gradients in the SLAC Disk-Loaded Structure," Stanford Linear Accelerator Center Report No. SLAC/AP-26 (1985).
16. J. W. Wang, V. Nguyen-Tuong, and G. A. Loew, "RF Breakdown Studies in a SLAC Disk Loaded Structure," these proceedings.
17. E. Tanabe, "Breakdown in High Gradient Accelerators," Gesellschaft fur Schwerionenforschung report No. GSI-84-11, 403 (1984).
18. A. H. McEuen et al., "High Power Operation of Accelerator Structures at Liquid Nitrogen Temperature," IEEE Trans. Nucl. Sci., NS-32, No. 5, 2972 (1985).